Supplementary Information

Band-gap engineering of BiOCl by oxygen vacancies for efficient photooxidation properties under visible-light irradiation

Dandan Cui,[a,b,c,⊥] Liang Wang,[b,c,⊥] Kang Xu,[a,c] Long Ren,[b,c] Li Wang,[b,c] Youxing Yu,[d,c] Yi Du,[a,b,c] and Weichang Hao*,[a,b,c]

[a]Department of Physics and Key Laboratory of Micro-Nano Measurement, Manipulation and Physics, Ministry of Education, Beihang University, Beijing 100191, China.

[b]Institute for Superconducting and Electronic Materials, University of Wollongong, NSW 2500, Australia.

[c]BUAA-UOW Joint Research Centre, Beihang University, Beijing 100191, China.

[d]School of Materials of Science and Engineering, Beihang University, Beijing 100191, China.

*Corresponding author: whao@buaa.edu.au

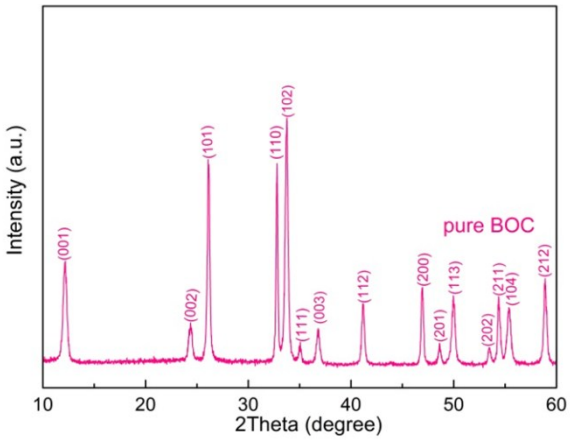

Fig. S1 XRD patterns of pure BOC.

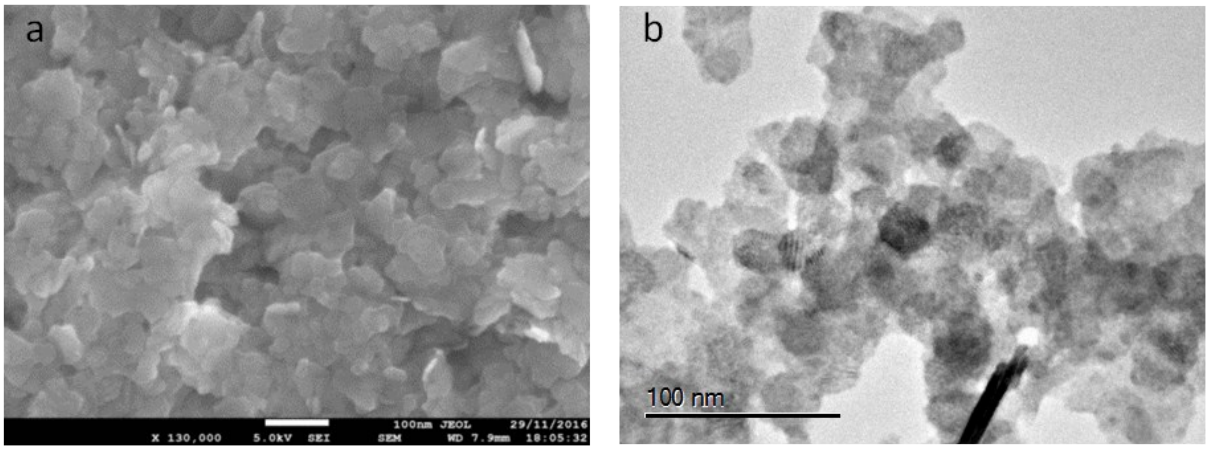

Fig. S2 (a) SEM and (b) TEM images of OV-rich BOC.

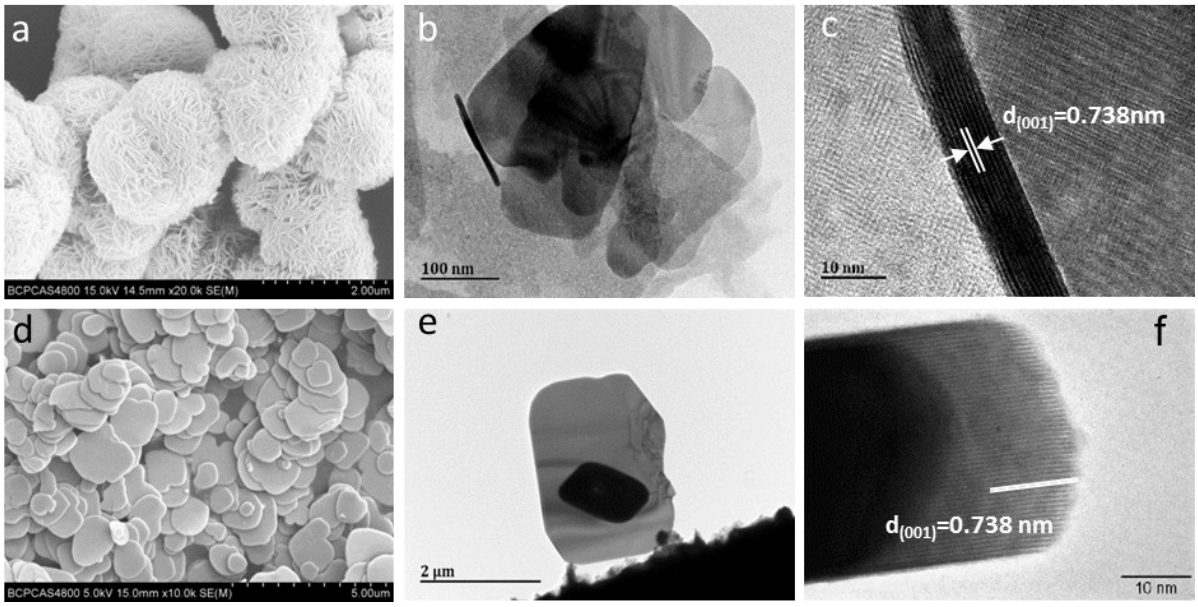

Fig. S3 SEM images of (a) OV-poor BOC and (d) pure BOC; planar-view TEM images of (b) OV-poor BOC and (e) pure BOC; side-view HRTEM images of (c) OV-poor BOC and (f) pure BOC.

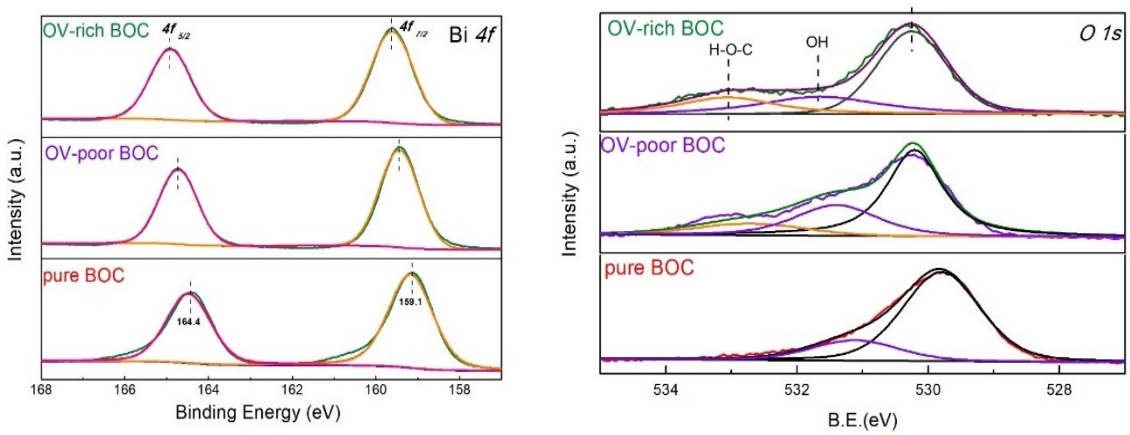

Fig. S4 (a) High-resolution XPS spectra of Bi 4f and (b) High-resolution XPS spectra of O 1s for the OV-rich, OV-poor and pure BOC samples.

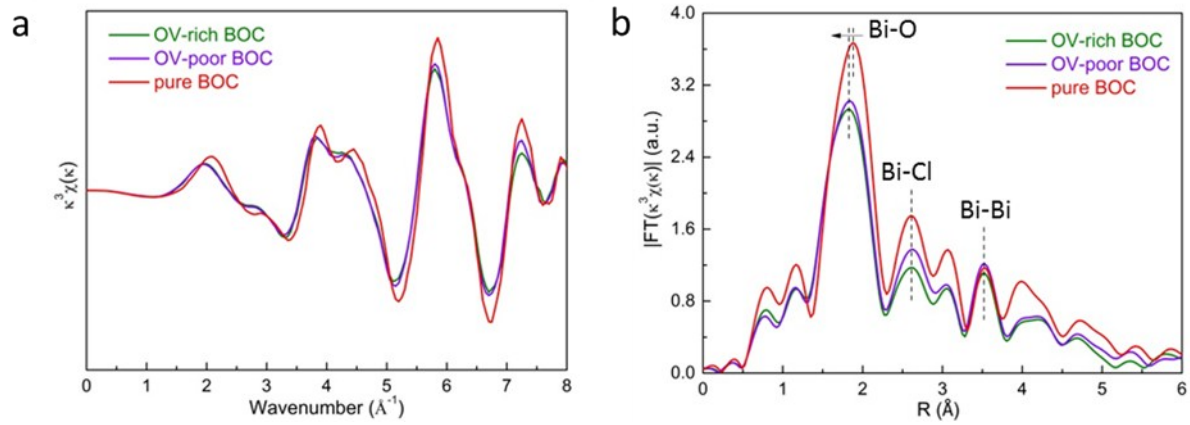

Fig. S5 (a) Bi L-edge extended XAFS oscillation function $\kappa^3\chi(\kappa)$ and (b) the corresponding Fourier transforms for the OV rich/poor BOC and pure BOC.

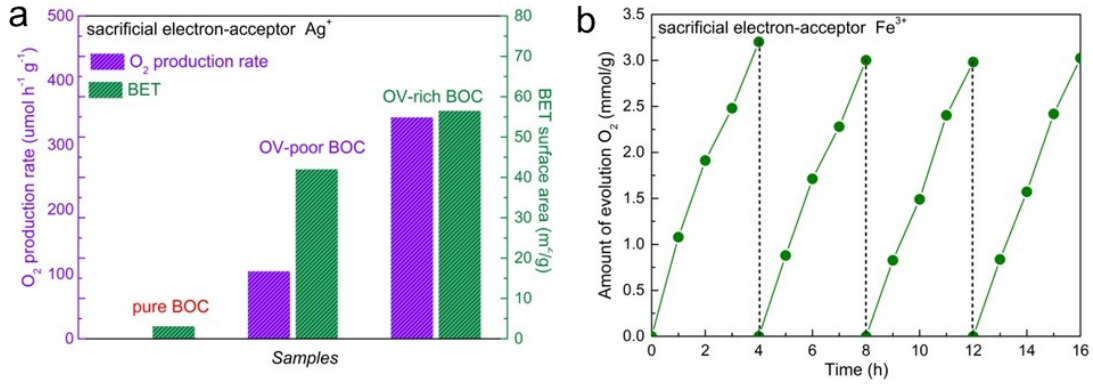

Fig. S6 (a) comparison of the photocatalytic O_2 production rate under visible-light irradiation ($\lambda \geq 420$ nm) over OV-rich/poor BOC and pure BOC. (b) Cycling test of O_2 production from water under visible-light irradiation ($\lambda \geq 420$ nm) over OV-rich BOC.

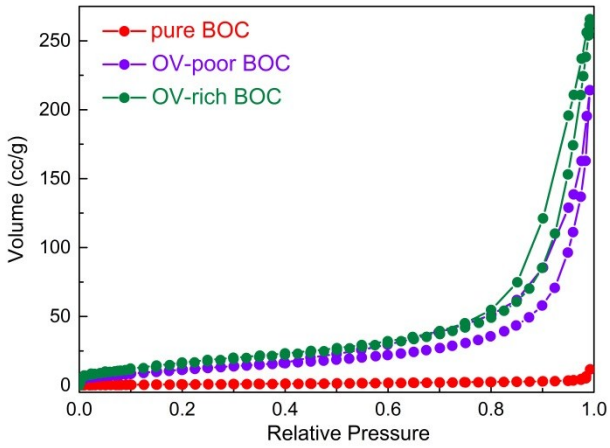

Fig. S7. Nitrogen adsorption–desorption isotherms of OV-rich/poor BOC and pure BOC.

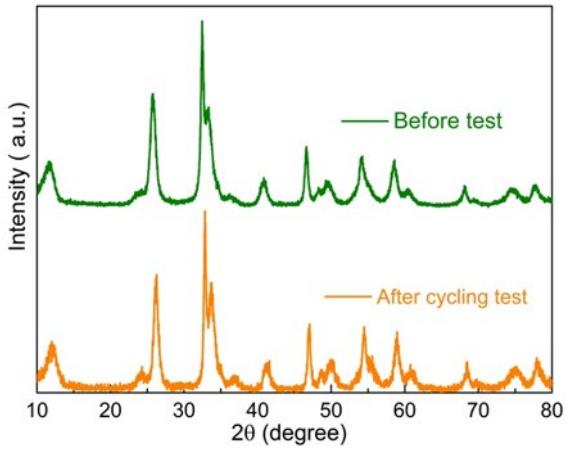

Fig. S8 XRD patterns of OV-rich BOC before and after the cycling test of O_2 evolution under visible light irradiation.

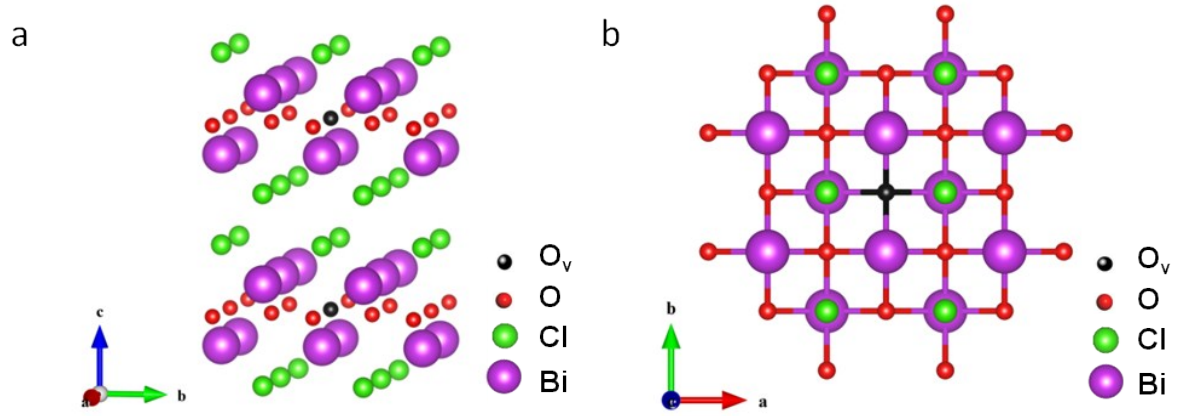

Fig. S9 Simulated crystal structure of BiOCl with oxygen vacancies: (a) side view and (b) top view of (001) facet.

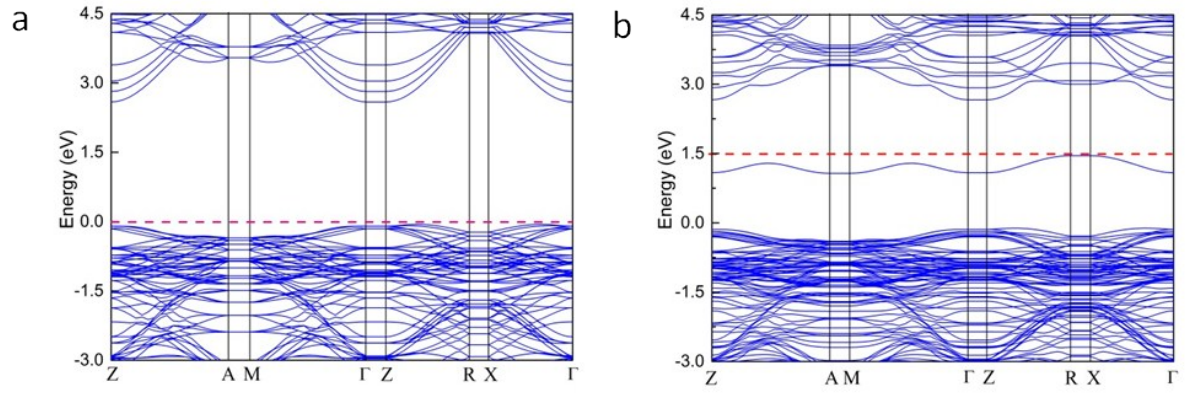

Fig. S10 Band structure of (a) perfect BiOCl and (b) BiOCl with oxygen vacancies.

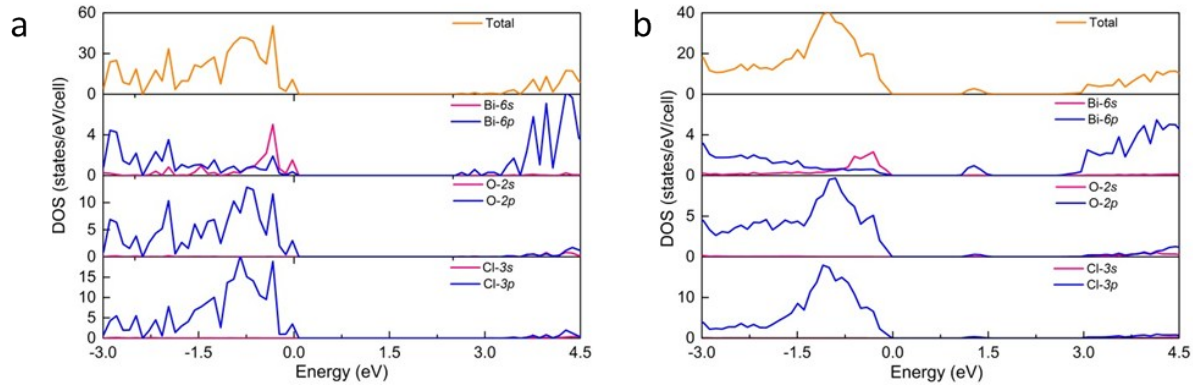

Fig. S11 Total and partial electronic density of states (DOS) of (a) perfect BiOCl and (b) BiOCl with oxygen vacancies.

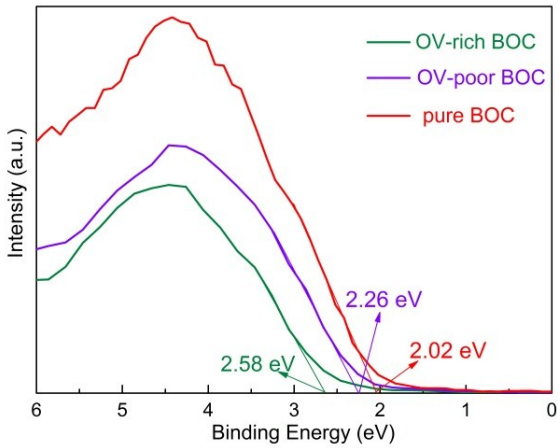

Fig. S12 XPS valence band spectra of OV-rich/poor BOC and pure BOC.